

# Reaction of sulfate and phosphate radicals with $\alpha,\alpha,\alpha$ -trifluorotoluene



Janina A. Rosso,<sup>a</sup> Patricia E. Allegretti,<sup>b</sup> Daniel O. Mártire<sup>a\*</sup> and Mónica C. Gonzalez<sup>a\*</sup>

<sup>a</sup> Instituto de Investigaciones Fisicoquímicas Teóricas y Aplicadas (INIFTA), Facultad de Ciencias Exactas, Universidad Nacional de La Plata, Casilla de Correo 16, Sucursal 4, (1900) La Plata, Argentina. E-mail: dmartire@volta.ing.unlp.edu.ar; fax: 00 54 21 25 4642

<sup>b</sup> Laboratorio de Estudio de Compuestos Orgánicos, División Química Orgánica, Facultad de Ciencias Exactas, Universidad Nacional de La Plata (1900) La Plata, Argentina

Received (in Cambridge) 6th October 1998, Accepted 11th November 1998

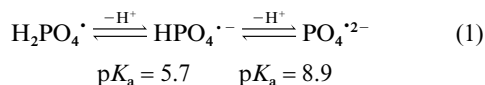
The aqueous phase reactions of  $\alpha,\alpha,\alpha$ -trifluorotoluene (TFT) with sulfate and phosphate radicals have been investigated by conventional flash-photolysis. The bimolecular rate constants obtained for the reactions of  $\text{SO}_4^{\cdot-}$ ,  $\text{H}_2\text{PO}_4^{\cdot}$ ,  $\text{HPO}_4^{\cdot-}$  and  $\text{PO}_4^{\cdot 2-}$  with TFT are  $(2 \pm 1) \times 10^7$ ,  $(3.5 \pm 0.5) \times 10^7$ ,  $(2.7 \pm 0.5) \times 10^6$  and  $(9 \pm 1) \times 10^5 \text{ M}^{-1} \text{ s}^{-1}$ , respectively. The organic radicals produced from these reactions exhibit a common absorption peak at 290–300 nm. Additionally, the transients generated from sulfate radicals show a shoulder at 360–370 nm and those generated from phosphate radicals a less intense maximum at 400 nm. Based on the experimental results, the nature of the organic radicals is discussed. Additional information on the hydroxycyclohexadienyl radicals of TFT is obtained from independent experiments with hydrogen peroxide solutions containing TFT.

## Introduction

A wide variety of reactions involving inorganic radical ions participate in the removal of relatively stable pollutants in the aqueous phase of our environment.

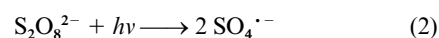
$\text{SO}_4^{\cdot-}$  is a chain carrier in the atmospheric oxidation of  $\text{SO}_2$ , and consequently is able to initiate the degradation of many of the compounds present in clouds and aerosols.<sup>1</sup>  $\text{SO}_4^{\cdot-}$  radical ions react with several aromatic compounds, either by addition to the benzene ring or by direct electron transfer from the ring to  $\text{SO}_4^{\cdot-}$ ,<sup>2</sup> yielding organic radicals, which upon further reaction lead to oxidation of the aromatics.

Phosphate ions are often present in high concentrations in agricultural and industrial waste water and they are of environmental concern.<sup>3</sup> Anthropogenic and natural generation of  $\text{SO}_4^{\cdot-}$  or  $\text{HO}^{\cdot}$  radicals in phosphate containing waste-water may give rise to the formation of three phosphate radicals ( $\text{H}_2\text{PO}_4^{\cdot}$ ,  $\text{HPO}_4^{\cdot-}$  and  $\text{PO}_4^{\cdot 2-}$ ) related by the acid–base equilibria shown in eqn. (1).<sup>4</sup> Phosphate radicals are known to react with several organic substrates,<sup>4–8</sup> their relative oxidation capabilities decreasing in the order:  $\text{SO}_4^{\cdot-} > \text{H}_2\text{PO}_4^{\cdot} > \text{HPO}_4^{\cdot-} > \text{PO}_4^{\cdot 2-}$ .<sup>5,7,8</sup>



A knowledge of the reaction mechanisms involved in  $\text{SO}_4^{\cdot-}$  and phosphate radical-initiated oxidation of organic pollutants is of importance for understanding the chemistry of our environment and for the optimisation of advanced technologies for waste-water treatment. Here, we report a mechanistic study of the aqueous phase reactions of sulfate and phosphate radicals with  $\alpha,\alpha,\alpha$ -trifluorotoluene (TFT). In particular, TFT is a flammable, corrosive reactant used in the manufacture of high polymer chemistry, in dielectric fluids and in dye chemistry, and consequently is of environmental concern.

Photolysis of  $\text{S}_2\text{O}_8^{2-}$  ( $\lambda_{\text{exc}} < 300 \text{ nm}$ ), reaction (2), is a clean



source of sulfate radical ions with pH-independent high quantum yields.<sup>9</sup> On the other hand, photolysis of  $\text{P}_2\text{O}_8^{4-}$  ( $\lambda_{\text{exc}} < 300 \text{ nm}$ ), reaction (3), has been reported to yield phosphate radical



ions.<sup>4,10,11</sup> Thus, the reactions of TFT with  $\text{SO}_4^{\cdot-}$ ,  $\text{H}_2\text{PO}_4^{\cdot}$ ,  $\text{HPO}_4^{\cdot-}$  and  $\text{PO}_4^{\cdot 2-}$  were studied by flash-photolysis of  $\text{S}_2\text{O}_8^{2-}$  or  $\text{P}_2\text{O}_8^{4-}$  solutions in the presence of TFT.

## Results

### $\text{S}_2\text{O}_8^{2-}$ experiments

**Experiments with  $[\text{TFT}] < 2.5 \times 10^{-4} \text{ M}$ .** Photolysis of aqueous peroxodisulfate solutions in the pH range 1–7 showed the formation of a transient species in the wavelength range from 300 to 550 nm, whose spectrum recorded immediately after the flash of light is in agreement with that reported in the literature for  $\text{SO}_4^{\cdot-}$ .<sup>9,12</sup> The kinetic analysis of the transient traces over more than three half-lives showed that the decay is fitted to simultaneous first and second order processes. The reaction rate constant for the second order process [ $2k = (1.6 \pm 0.5) \times 10^9 \text{ M}^{-1} \text{ s}^{-1}$ ]† is of the order reported for the bimolecular recombination of  $\text{SO}_4^{\cdot-}$ .<sup>9</sup> The weight factor of each process strongly depends on the irradiation light intensity and peroxodisulfate concentration. In experiments with low flash intensity and  $[\text{S}_2\text{O}_8^{2-}] = 5 \times 10^{-3} \text{ M}$ , the sulfate radical ion was observed to decay mainly by a first order process in fractions of milliseconds, as expected from the reaction between sulfate radical ions and  $\text{S}_2\text{O}_8^{2-}$  ions yielding  $\text{S}_2\text{O}_8^{\cdot-}$  radicals.<sup>9</sup>

Experiments with  $[\text{S}_2\text{O}_8^{2-}] = 5.04 \times 10^{-3} \text{ M}$  and  $[\text{TFT}] < 2.5 \times 10^{-4} \text{ M}$  show absorption traces at  $\lambda > 350 \text{ nm}$ , whose spectrum immediately after the flash of light agrees with that of  $\text{SO}_4^{\cdot-}$ .

† The error bars are in all cases considered for a 99% confidence level.

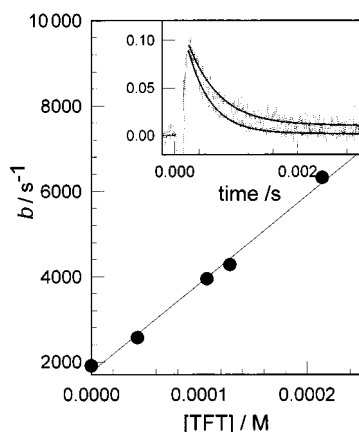
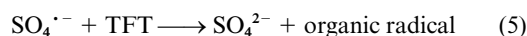


**Fig. 1** Linear dependence of  $b$  on  $[TFT]$  obtained for  $\lambda = 450$  nm. Inset: signals obtained at  $\lambda = 450$  nm from  $5.04 \times 10^{-3}$  M  $S_2O_8^{2-}$  solutions in the absence (upper trace) and presence (lower trace) of  $4.28 \times 10^{-5}$  M TFT. The solid lines indicate the fitting functions.

The experimental absorption traces at a given observation wavelength,  $A(\lambda)$ , could be well fitted according to eqn. (4), as

$$A(\lambda) = a(\lambda) \exp(-bt) + c(\lambda) \quad (4)$$

shown in Fig. 1 (inset). The calculated constant  $b$  is independent on the detection wavelength and linearly depends on  $[TFT]$  (Fig. 1), as expected for the reaction of  $SO_4^{\cdot-}$  with TFT [reaction (5)]. The constant term  $c(\lambda)$ , associated with the absorption



of a longer lived species formed following  $SO_4^{\cdot-}$  depletion, is less than 6% the initial absorption of  $SO_4^{\cdot-}$  [pre-exponential factor  $a(\lambda)$ ] and could not be accurately determined from these fittings.

From the slope of the straight line shown in Fig. 1, the bimolecular rate constant for reaction (5),  $k_5 = (2 \pm 1) \times 10^7$  M<sup>-1</sup> s<sup>-1</sup>, is obtained. The observed rate constant is lower than that reported for the reaction between the electrophilic  $SO_4^{\cdot-}$  radical and other substituted benzenes (except for nitrobenzene), as expected from the stronger electron withdrawing ability of  $CF_3$ .<sup>13,14</sup>

**Experiments with  $[TFT] \geq 5 \times 10^{-4}$  M.** For irradiation experiments with  $[S_2O_8^{2-}] = 5.0 \times 10^{-3}$  M and  $[TFT] \geq 5 \times 10^{-4}$  M, reaction (5) is very efficient and  $SO_4^{\cdot-}$  radicals are readily scavenged, and thus not observed within our time resolution. Under these conditions, formation of transient species absorbing in the wavelength region from 250 to 450 nm was observed for air and nitrogen-saturated solutions of pH 1, 2.5 and 7. Blank experiments performed with TFT solutions in the absence of  $S_2O_8^{2-}$ , but otherwise identical experimental conditions, showed no signal, thus indicating that the observed transients are mainly formed after reaction (5) rather than by photolysis of TFT.

The observed traces exhibit a fast absorbance depletion and a final constant absorbance, as shown in Fig. 2 for a typical experiment, thus indicating the formation of short-lived intermediates and stable reaction products. The absorption spectrum of the short-lived transients and that of the stable products are shown in Fig. 3. Absorption spectra taken several minutes after flash irradiation were similar to those shown in Fig. 3 inset.

The time dependence of the experimental traces obtained at each analysis wavelength,  $\lambda$ , in the range from 250 to 330 nm, could be well fitted to eqn. (6), as shown by the solid lines in Fig. 2.

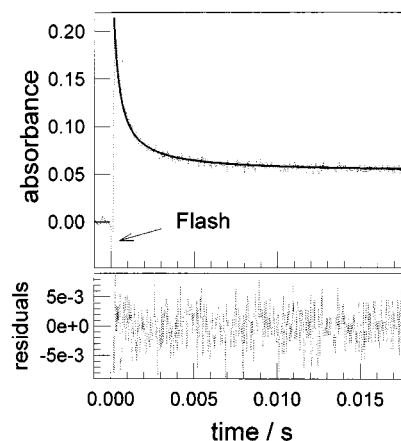


**Fig. 2** Signal obtained at  $\lambda = 300$  nm from nitrogen-saturated  $5 \times 10^{-3}$  M  $S_2O_8^{2-}$  solutions in the presence of  $5.2 \times 10^{-4}$  M TFT at pH 2.6. The solid line indicates the fitting function.

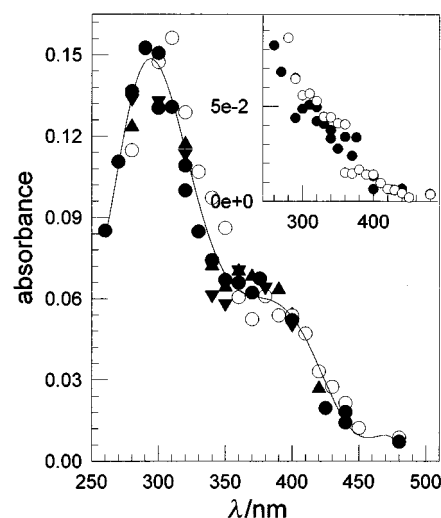


**Fig. 3** Absorption spectrum of the transients observed 300  $\mu$ s after the flash irradiation of  $5 \times 10^{-3}$  M  $S_2O_8^{2-}$  in the presence of  $5.2 \times 10^{-4}$  M TFT. Air-saturated solutions of pH 1 ( $\blacktriangle$ ), 2.6 ( $\bullet$ ) and 7 ( $\blacktriangledown$ ). Nitrogen-saturated solutions of pH 2.6 ( $\circ$ ). Inset: absorption spectrum observed 20 ms after flash irradiation of air- ( $\bullet$ ) and nitrogen- ( $\circ$ ) saturated solutions of pH = 2.6.

$$A(\lambda) = \frac{1}{d(\lambda) + f(\lambda)t} + g(\lambda) \quad (6)$$

The values of  $d(\lambda)$ ,  $f(\lambda)$  and  $g(\lambda)$  are constant at each  $\lambda$  and are, within experimental error, independent of pH and on the presence of molecular oxygen. Moreover, the values for  $f(\lambda)$  are almost insensitive to the incident light intensity and to the concentrations of  $S_2O_8^{2-}$  and TFT for  $[TFT] \geq 5 \times 10^{-4}$  M. As the optical pathlength  $l$  is 20 cm, the value  $2k_{BR}/\epsilon_{T(300\text{ nm})} = (4.0 \pm 1.5) \times 10^5$  cm s<sup>-1</sup> is obtained for the bimolecular decay rate constant of the transient absorbing below 330 nm.

On the other hand, the experimental traces obtained for  $\lambda > 330$  nm are oxygen sensitive, as faster absorbance depletion rates are observed for air than for nitrogen saturated solutions. Thus, the traces at  $\lambda > 330$  nm should correspond to a different transient than that exhibiting an absorption maximum at 280–300 nm.

#### $P_2O_8^{4-}$ experiments

**Experiments with  $[TFT] < 5 \times 10^{-4}$  M.** Photolysis of air-saturated aqueous solutions of peroxodiphosphate at pH 4.0, 7.1 and 10.1 showed the formation of transient species in the wavelength range from 300 to 600 nm, whose spectra are in agreement with those reported in the literature for  $H_2PO_4^{\cdot}$ ,  $HPO_4^{\cdot-}$  and  $PO_4^{\cdot 2-}$ , respectively.<sup>7,12</sup> Similar experiments but

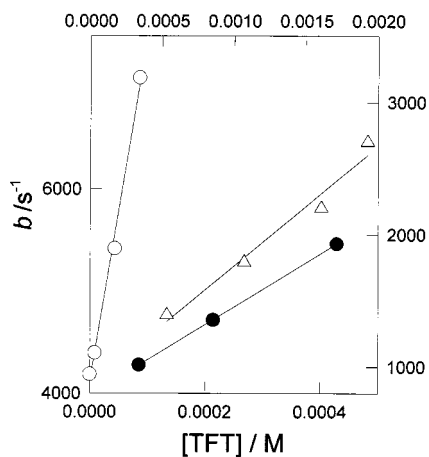
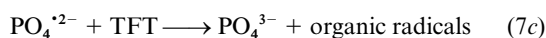
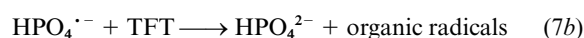
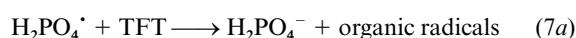


**Fig. 4** Linear dependence of  $b$  on  $[TFT]$  obtained for  $\lambda = 500$  nm for  $H_2PO_4^\bullet$  (○, left Y-axis and lower X-axis),  $HPO_4^{\bullet-}$  (△, right Y-axis and lower X-axis) and  $PO_4^{\bullet 2-}$  radicals (●, right Y-axis and upper X-axis).

with added  $[TFT] < 5 \times 10^{-4}$  M at each pH showed absorption traces at  $\lambda > 400$  nm, whose spectra also agreed with those of the corresponding phosphate radicals. The experimental traces could be well fitted according to eqn. (4). The calculated constant  $b$  is independent of  $\lambda$  and linearly depends on  $[TFT]$  (Fig. 4), as expected for the reaction of phosphate radicals with TFT, reactions (7a), (7b) and (7c). The very small remaining



absorption [constant term  $c(\lambda)$ ] can be associated with a longer lived species formed following phosphate radical depletion.

The slopes of the plots shown in Fig. 4 yield the bimolecular rate constants  $k_{7a} = (3.4 \pm 0.5) \times 10^7$  M<sup>-1</sup> s<sup>-1</sup>,  $k_{7b} = (2.7 \pm 0.5) \times 10^6$  M<sup>-1</sup> s<sup>-1</sup> and  $k_{7c} = (9 \pm 1) \times 10^5$  M<sup>-1</sup> s<sup>-1</sup> for the reaction of  $H_2PO_4^\bullet$ ,  $HPO_4^{\bullet-}$  or  $PO_4^{\bullet 2-}$  radicals with TFT, respectively. The measured values are in agreement with those expected from the reported correlation of rate constants vs. Hammett substituent constant,  $\sigma$ , for reactions involving each of the three acid-base forms of phosphate radicals and substituted benzenes.<sup>7,8</sup>

**Experiments with  $[TFT] > 5 \times 10^{-4}$  M.** For irradiation experiments with air- and nitrogen-saturated peroxodiphosphate solutions of pH 4.0 and 7.1 in the presence of  $[TFT] > 5 \times 10^{-4}$  M,  $H_2PO_4^\bullet$  and  $HPO_4^{\bullet-}$  radicals are readily depleted and formation of transient species absorbing in the wavelength region from 250 to 450 nm is observed. The traces show fast absorbance depletion and a final constant absorbance, as observed for the experiments with  $S_2O_8^{2-}$ , indicating the formation of short lived intermediates and stable products. The absorption spectrum observed at both pH values are, within experimental error, identical and independent of the presence of molecular oxygen, as shown in Fig. 5.

The traces can be well fitted according to eqn. (6). The value  $2k_{BR}/\epsilon_{T(300\text{ nm})} = (3.0 \pm 1.5) \times 10^5$  cm s<sup>-1</sup> is obtained for the bimolecular decay rate constant for the observed transient.

As reaction (7c) is not efficient, the traces obtained from solutions of pH 10 show important absorbance contributions due to  $PO_4^{\bullet 2-}$  radicals, even for saturated aqueous solutions of TFT. Consequently, these traces were not further analysed.

#### Characterisation of hydroxycyclohexadienyl (HCHD) radicals of TFT

$HO^\bullet$  radicals react with aromatic substrates by electrophilic

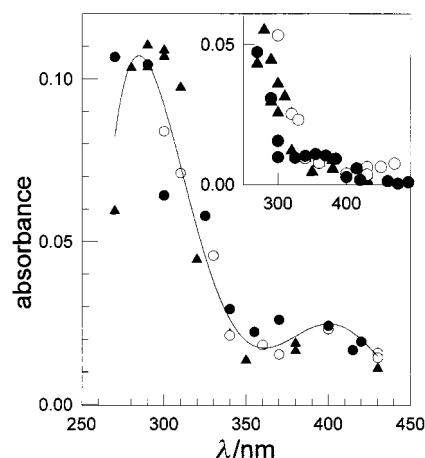
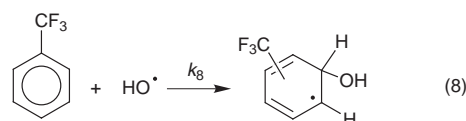
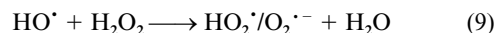


**Fig. 5** Absorption spectrum of the transients obtained 300  $\mu$ s after the flash irradiation of  $3 \times 10^{-3}$  or  $3 \times 10^{-4}$  M  $P_2O_8^{4-}$  (for solutions of pH 4 and 7, respectively) in the presence of TFT ( $> 5.2 \times 10^{-4}$  M). Air-saturated solutions of pH 4 (▲) and 7 (●). Nitrogen-saturated solutions of pH 7 (○). Inset: corresponding absorption spectrum observed 20 ms after flash irradiation.

addition to the aromatic ring yielding HCHD radicals, reaction (8).<sup>15b,16,17</sup> In particular, TFT was reported to react with  $HO^\bullet$



radicals yielding reaction products derived from the initial formation of HCHD radicals of TFT.<sup>18</sup> For the purpose of generating HCHD radicals of TFT, nitrogen- and air-saturated  $5 \times 10^{-4}$  M hydrogen peroxide solutions containing  $1.3 \times 10^{-3}$  M TFT were irradiated. Reaction between  $HO^\bullet$  radicals and hydrogen peroxide, reaction (9), yielding  $HO_2^\bullet$  and  $O_2^{\bullet-}$  can be

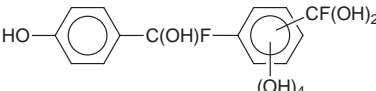
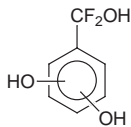
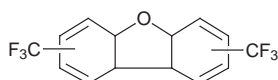


neglected under our experimental conditions since  $v_8 \gg v_9$ ,<sup>19,20</sup> where  $v$  stands for the reaction rate.

Formation of transient species absorbing in the wavelength region from 250 to 350 nm was observed, both in the presence and absence of molecular oxygen. The traces show a fast absorbance depletion and a final constant absorbance, indicating the formation of short lived intermediates and stable products after reaction (8). Both absorption spectra are shown in Fig. 6. The traces obtained at different observation wavelengths could be well fitted to eqn. (6). The values of  $d(\lambda)$ ,  $f(\lambda)$  and  $g(\lambda)$  are, within experimental error, independent of the presence of molecular oxygen. A recombination rate constant  $2k_{BR}/\epsilon_{T(290\text{ nm})} = (6 \pm 4) \times 10^5$  cm s<sup>-1</sup> is estimated for these transients.

HCHD radicals are known to present a single absorption maximum at around 300–310 nm<sup>15,21</sup> with absorption coefficients  $\geq 2000$  M<sup>-1</sup> cm<sup>-1</sup>. In the absence of molecular oxygen they disproportionate and/or dimerise yielding phenols and biphenyls, respectively.<sup>18,22</sup> The bimolecular decay rates,  $2k_{BR}/\epsilon_{\text{max}}$ , lie in the range from  $1 \times 10^5$  to  $5 \times 10^5$  s<sup>-1</sup> cm for a wide range of substituted HCHD radicals.<sup>17,21,23–25</sup> HCHD radicals have been shown to react reversibly with molecular oxygen yielding peroxy radicals, which exhibit only broad absorption at  $\lambda < 300$  nm.<sup>8,26</sup> Considerable electron-density at the carbon atom is required for the formation of C–OO<sup>•</sup> bonds of peroxy radicals. Consequently, HCHD radicals containing strong electron-attracting groups, such as CN, do not show formation of peroxy radicals.<sup>16</sup> As the  $CF_3$  group is a stronger electron withdrawing substituent than CN,<sup>14</sup> behaviour similar to that reported for the HCHD radical of benzonitrile is expected for the HCHD radical of TFT.

**Table 1** Products identified under different experimental conditions

Tentative structure	GC retention time (RT/min) and important mass peaks [ <i>m/z</i> (%)]	Experimental conditions
(1) 	(RT 16.3) 347(4.3); 346(M <sup>+</sup> , 12.0); 329([M - OH] <sup>+</sup> , 15.0); 328([M - H <sub>2</sub> O] <sup>+</sup> , 9.5); 327([M - F] <sup>+</sup> , 8.5); 315([M - CF] <sup>+</sup> , 8.5); 281([M - CF(OH)] <sup>+</sup> , 9.2); 254([M - PhO] <sup>+</sup> , 32.2); 253([M - PhOH] <sup>+</sup> , 100); 195(15.0); 177(10.2); 93([PhOH] <sup>+</sup> , 27.9); 67(15.4); 41(20.7)	[H <sub>2</sub> O <sub>2</sub> ] = 1 M and [TFT] = 8 × 10 <sup>-4</sup> M; [S <sub>2</sub> O <sub>8</sub> <sup>2-</sup> ] = 4.5 × 10 <sup>-3</sup> M and [TFT] = 1.3 × 10 <sup>-3</sup> M; [P <sub>2</sub> O <sub>8</sub> <sup>4-</sup> ] = 2.3 × 10 <sup>-4</sup> M and [TFT] = 1.3 × 10 <sup>-3</sup> M
(2) 	(RT 2.6) 176([M] <sup>+</sup> , 56.9); 159([M - OH] <sup>+</sup> , 8.5); 158([M - H <sub>2</sub> O] <sup>+</sup> , 19.5); 141([M - H <sub>2</sub> O-HO] <sup>+</sup> , 9.7); 127([M - CH <sub>2</sub> FOH] <sup>+</sup> , 62.3); 109([M - CF <sub>2</sub> OH] <sup>+</sup> , 8.3); 49([C(OH)HF] <sup>+</sup> , 100)	[TFT] = 2.0 × 10 <sup>-3</sup> M
(3) 	(RT 13.8) 308([M] <sup>+</sup> , 15.4); 307([M - H] <sup>+</sup> , 35.2); 289([M - F] <sup>+</sup> , 65.4); 277([M - CF] <sup>+</sup> , 13.2); 258([M - CF <sub>2</sub> ] <sup>+</sup> , 42.7); 239([M - CF <sub>3</sub> ] <sup>+</sup> , 28.4); 163([M - C <sub>6</sub> H <sub>5</sub> CF <sub>3</sub> ] <sup>+</sup> , 100); 77([Ph] <sup>+</sup> , 57.3); 69([CF <sub>3</sub> ] <sup>+</sup> , 15.4)	[TFT] = 2.0 × 10 <sup>-3</sup> M
(4) HCOC(CH <sub>3</sub> )OH(CHOH) <sub>3</sub> -CHO	(RT 2.4) 103([HOCC(CH <sub>3</sub> )OHCH=OH] <sup>+</sup> , 6.5); 101 ([CH=C(OH)CHOHCOH] <sup>+</sup> , 15.0); 89([HOCCHOHCH=OH] <sup>+</sup> , 10.0); 85([103 - H <sub>2</sub> O] <sup>+</sup> , 8.5); 73([HOCC(CH <sub>3</sub> )=OH] <sup>+</sup> , 36.6); 60([CH(OH)CH=OH] <sup>+</sup> , 9.5); 75([CH <sub>3</sub> C=CH(OH) - OH] <sup>+</sup> , 5.4); 57([75 - H <sub>2</sub> O] <sup>+</sup> , 8.6); 55([73 - H <sub>2</sub> O] <sup>+</sup> , 16.2); 45([73 - CO] <sup>+</sup> , 100); 42([60 - H <sub>2</sub> O] <sup>+</sup> , 19.3)	[H <sub>2</sub> O <sub>2</sub> ] = 1 M and [TFT] = 8 × 10 <sup>-4</sup> M; [S <sub>2</sub> O <sub>8</sub> <sup>2-</sup> ] = 0.044 M and [TFT] = 8 × 10 <sup>-4</sup> M
(5) (CH <sub>3</sub> )CO-(CHOH) <sub>2</sub> -CHO	(RT 2.8) 89([HCOC(OH)=C=OH] <sup>+</sup> , 12.0); 88(8.9); 74(5.4); 73([CH <sub>3</sub> C(OH)=COH] <sup>+</sup> , 16.1); 71([89 - H <sub>2</sub> O] <sup>+</sup> , 5.9); 61(9.2); 59([74 - CH <sub>3</sub> ] <sup>+</sup> , 10.4); 43([CH <sub>3</sub> CO] <sup>+</sup> , 100); 41([59 - H <sub>2</sub> O] <sup>+</sup> , 78.4)	[H <sub>2</sub> O <sub>2</sub> ] = 1 M and [TFT] = 8 × 10 <sup>-4</sup> M; [S <sub>2</sub> O <sub>8</sub> <sup>2-</sup> ] = 0.044 M and [TFT] = 8 × 10 <sup>-4</sup> M; [P <sub>2</sub> O <sub>8</sub> <sup>4-</sup> ] = 2.3 × 10 <sup>-3</sup> M and [TFT] = 8 × 10 <sup>-4</sup> M
(6) HCOCHOHC(CH <sub>3</sub> )OH(CHOH) <sub>2</sub> CHO	(RT 3.4) 133([M - HOCCH(OH)] <sup>+</sup> , 15.0); 115([133 - H <sub>2</sub> O] <sup>+</sup> , 8.4); 89([CHO=CHCH(OH)CH(OH)COH] <sup>+</sup> , 27.2); 71([89 - H <sub>2</sub> O] <sup>+</sup> , 62.3); 61([H <sub>2</sub> OCH=CHOH] <sup>+</sup> , 57.2); 59([HOCCH=OH] <sup>+</sup> , 16.5); 45([HOCHCH <sub>3</sub> ] <sup>+</sup> , 70.3); 43([61 - H <sub>2</sub> O] <sup>+</sup> , 100)	[S <sub>2</sub> O <sub>8</sub> <sup>2-</sup> ] = 0.044 M and [TFT] = 8 × 10 <sup>-4</sup> M; [P <sub>2</sub> O <sub>8</sub> <sup>4-</sup> ] = 2.3 × 10 <sup>-3</sup> M and [TFT] = 8 × 10 <sup>-4</sup> M

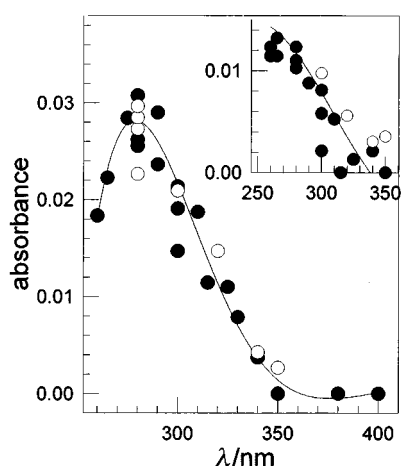


**Fig. 6** Absorption spectrum of the transients obtained at 300 μs after the flash irradiation of air (●) and nitrogen (○) saturated 5 × 10<sup>-4</sup> M hydrogen peroxide solutions containing 1.3 × 10<sup>-3</sup> M TFT. Inset: corresponding absorption spectrum observed 20 ms after flash irradiation.

A blue shift in  $\lambda_{\max}$  with respect to other HCHD radicals<sup>15b</sup> and negligible contribution of the reaction of HCHD with molecular oxygen are expected for the electron withdrawing substituent CF<sub>3</sub>, as observed experimentally. Moreover, the bimolecular decay rate constant  $2k_{\text{BR}}/\epsilon_{\text{T}}(290 \text{ nm})$  is of the same order as those reported for other substituted HCHD radicals. Consequently, the observed transient species is assigned to an isomeric mixture of HCHD radicals of TFT.

### Product analysis

Identification of the products formed after the reactions of

TFT with SO<sub>4</sub><sup>-•</sup>, HO<sup>•</sup> and phosphate radicals in air-saturated solutions was attempted. Since TFT photolysis has been reported to yield oxidised photoproducts,<sup>18</sup> blank experiments with TFT solutions in the absence of oxidants without filtering the flash light were performed. Otherwise, all experiments for product analysis were done under identical experimental conditions to those used in the time-resolved experiments.

The tentative structures of the observed products are shown in Table 1. Almost the same products were observed to be formed in experiments with S<sub>2</sub>O<sub>8</sub><sup>2-</sup> or P<sub>2</sub>O<sub>8</sub><sup>4-</sup> for similar [TFT] to [S<sub>2</sub>O<sub>8</sub><sup>2-</sup>] or [P<sub>2</sub>O<sub>8</sub><sup>4-</sup>] ratios. Formation of a polymeric structure [product (1)] was observed in flash experiments with [TFT] to [oxidant] ratios > 0.3. Experiments with H<sub>2</sub>O<sub>2</sub> also showed formation of product (1), but for much lower [TFT] to [H<sub>2</sub>O<sub>2</sub>] ratios. TFT photolysis yields product (2) and a dibenzofuran derivative of TFT [product (3)]. Experiments with [TFT] to [oxidant] ratios ≤ 0.3 showed formation of hydroxylated open chain products of 5 or 7 C atoms, not containing fluorine in their structures [products (4), (5) and (6)]. Complete consumption of the reactant after three flashes of light was observed for the latter experiments.

Hydroxylation reactions occur both on the aromatic ring and on the side-chain. The observed defluorination is in agreement with the measured F<sup>-</sup> concentration (~3 × 10<sup>-5</sup> M) observed after irradiating TFT solutions containing S<sub>2</sub>O<sub>8</sub><sup>2-</sup> or P<sub>2</sub>O<sub>8</sub><sup>4-</sup> with three flashes.

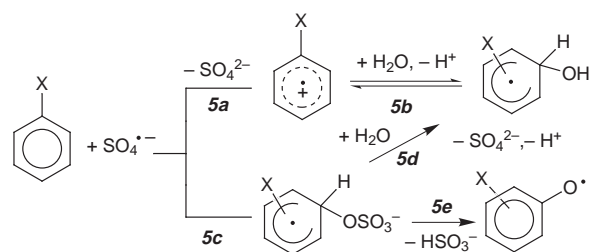
The high degree of oxidation observed in the products identified suggests that important thermal reactions following the primary reactions (5), (7) and (8), are taking place. In fact, photo-products (2) and (3) present in photolysed solutions of TFT were almost quantitatively converted to higher oxidised derivatives when mixed with ca. 1 × 10<sup>-3</sup> M S<sub>2</sub>O<sub>8</sub><sup>2-</sup> or P<sub>2</sub>O<sub>8</sub><sup>4-</sup> for

half an hour (time required for the workout of the samples before chromatographic analysis).

An unusual susceptibility to hydrolysis has been reported for the  $\text{CF}_3$  group in *o*- and *p*-hydroxybenzene, which was ascribed to the weakening of the C–F bond by “no-bond” resonance and intramolecular H-bonding, yielding a quinoid structure with loss of HF.<sup>27</sup> When treated with dilute alkali, *p*- $\text{CF}_3$  phenol was reported to furnish higher polymers, presumably of the type  $[-\text{O}-\text{C}_6\text{H}_4-\text{CF}_2-]_n$ , *ortho*- isomers yield salicylic acid and *meta*- isomers are stable even under stringent conditions.<sup>27</sup> On the other hand, peroxodisulfate has been reported to efficiently introduce a second HO function to hydroxybenzotrifluorides in dilute alkali.<sup>28</sup> Consequently,  $\text{CF}_3$  hydrolysis, polyhydroxylation of the aromatic ring and polymerisation, as observed in product (1), can be due to subsequent thermal reactions if the primary products of oxidation present HO groups *para*- and/or *ortho* to  $\text{CF}_3$  in the aromatic ring.

## Discussion

Substituted benzenes have been suggested to react with  $\text{SO}_4^{\cdot-}$  radicals either by electron transfer from the aromatic ring to  $\text{SO}_4^{\cdot-}$  or by addition/elimination, as shown in Scheme 1. The



Scheme 1

value of  $k_5$  is well correlated with the Hammett type plot for reactions between  $\text{SO}_4^{\cdot-}$  and substituted benzenes yielding  $\rho = -2.4$ .<sup>13</sup> Such values of  $\rho$  were suggested to indicate that  $\text{SO}_4^{\cdot-}$  radicals react with high selectivity with substituted benzenes, most likely by an electron transfer mechanism initially producing the radical cation [reaction (5a) in Scheme 1].<sup>13</sup> The radical cation undergoes a fast reversible hydration to yield HCHD radicals [reaction (5b)], if no other reaction pathway is available.<sup>2,13,25</sup> However, an addition pathway yielding a  $\text{SO}_4^{\cdot-}$  adduct of TFT [reaction (5c)] followed by elimination of  $\text{SO}_4^{\cdot-}$  [reaction (5d)] or  $\text{SO}_3^{\cdot-}$  [reaction (5e)] yielding HCHD or phenoxy radicals, respectively, cannot be neglected.

At least two different transient species are formed after reaction of TFT with  $\text{SO}_4^{\cdot-}$ . The transient with maximum at around 290–300 nm shows absorption and kinetic properties very similar to those found for HCHD radicals of TFT, thus suggesting the contribution of these radicals, as expected from the proposed reaction scheme. Phenoxy radicals exhibit absorption with a maximum around 400 nm. However, they are unreactive towards  $\text{O}_2$ ; thus, the oxygen sensitive transient absorbing at around 370 nm cannot be assigned to these radicals.

Any contribution of the  $\text{SO}_4^{\cdot-}$  adducts of TFT to the observed spectrum can be neglected since these adducts have lifetimes shorter than 100 ns due to their fast hydrolysis reactions.<sup>2,15</sup>

Radical cations exhibit absorption in the wavelength range 325–390 nm. However, their contribution to the observed spectrum can also be neglected, since they present lifetimes of the order of the milliseconds only in acidic solutions,<sup>7,24,25,29</sup> in disagreement with the observed pH independence of the absorption traces. Alternative reaction paths, such as proton<sup>2</sup> or fluorine atom detachment from the radical cation of TFT, may give rise to the transients absorbing at  $\lambda > 330$  nm. The

latter suggestion is also supported by the defluorination observed in the identified reaction products.

Further reactions of the organic radicals with peroxodisulfate,<sup>30</sup> do not contribute to transient formation, since the transient spectra and decay kinetics are independent of  $[\text{S}_2\text{O}_8^{2-}]$ .

The observed experimental facts suggest that an electron transfer pathway as that shown in reaction (5a) is an important channel for the reaction between TFT and  $\text{SO}_4^{\cdot-}$ .

The  $\rho$  values determined from the Hammett correlation of rate constants for reactions involving substituted benzenes and  $\text{H}_2\text{PO}_4^{\cdot}$  or  $\text{HPO}_4^{\cdot-}$  radicals ( $\rho = -1.2$  and  $-1.3$ , respectively)<sup>7</sup> are within those reported for corresponding reactions with  $\text{SO}_4^{\cdot-}$  radicals ( $\rho = -2.4$ <sup>13</sup>) and with  $\text{HO}^{\cdot}$  radicals ( $\rho = -0.5$ <sup>20</sup>). The latter values of  $\rho$  were suggested to support the occurrence of addition reactions rather than electron transfer.<sup>15b,29</sup>

The spectrum of the organic transients formed from the reaction of TFT with  $\text{H}_2\text{PO}_4^{\cdot}$  or  $\text{HPO}_4^{\cdot-}$  radicals (Fig. 5) show absorption maxima at around 290–300 nm and a less intense one at 400 nm. Phenoxy radicals show characteristic absorption peaks at around 300 nm and lower maxima at around 400 nm. The absorption band observed at 400 nm showing a decay lifetime of the order of milliseconds, insensitive to oxygen concentration, could be due to the formation of an isomeric mixture of phenoxy radicals of TFT.<sup>21,31</sup> However, the band at 290–300 nm could arise from the contribution of both HCHD and phenoxy radicals, since this band also shows absorption and kinetic properties very similar to those found for HCHD radicals of TFT.

According to the preceding discussion,  $\text{H}_2\text{PO}_4^{\cdot}$  or  $\text{HPO}_4^{\cdot-}$  radical addition to the aromatic ring of TFT seems to be an important pathway for reactions (7). These reactions might form a phosphate radical adduct which, upon fast hydrolysis, eliminates either  $\text{HPO}_4^{3-}$  or  $\text{HPO}_3^{2-}$ , yielding hydroxycyclohexadienyl or phenoxy radicals, respectively. Such a reaction scheme parallels that proposed for  $\text{SO}_4^{\cdot-}$  radical ions [reactions (5c) to (5e) in Scheme 1] and is in agreement with other studies involving  $\text{HPO}_4^{\cdot-}$  radical reactions with chlorobenzene and phenol.<sup>8</sup>

Hydrogen-atom abstraction from the aromatic ring yielding reactive phenyl radicals is a further possibility. Phenyl radicals readily react with molecular oxygen to yield aryl peroxy radicals absorbing at around 400–500 nm.<sup>32</sup> In neutral solution, peroxy radicals decay by bimolecular recombination with rate constants  $< 10^7 \text{ M}^{-1} \text{ s}^{-1}$ ,<sup>8,32b</sup> and consequently, they are suitable for detection with our experimental set-up. However, the independence on oxygen concentration of the observed spectra does not seem to support the occurrence of such reactions.

Due to efficient thermal reactions following the primary oxidation steps, only ambiguous information on the reaction mechanisms can be obtained from the chromatographic analysis of the reaction products. However, as previously discussed, the primary products of oxidation might contain HO groups *para*- and/or *ortho*- to  $\text{CF}_3$  in the aromatic ring. As phenol type products are formed from the bimolecular disproportionation of HCHD radicals,<sup>33</sup> these observations are in agreement with HCHD being formed after reactions (5), (7) and (8).

Though  $\text{HO}^{\cdot}$ ,  $\text{SO}_4^{\cdot-}$ ,  $\text{H}_2\text{PO}_4^{\cdot}$  and  $\text{HPO}_4^{\cdot-}$  radical reactions with TFT are not very efficient, the subsequent thermal reactions of the products formed during the primary oxidation steps lead to the formation of less harmful, highly oxidised derivatives, as complete defluorination and rupture of the aromaticity was observed. These results are of importance for the evaluation of the environmental impact of TFT and related substances.

## Experimental

Hydrogen peroxide (Riedel de Haën), TFT (Fluka) and potassium peroxodisulfate (Riedel de Haën) were used as received.

Potassium peroxodiphosphate was prepared following the literature procedures.<sup>34</sup> Distilled water was passed through a Millipore system.

Flash-photolysis experiments were carried out in a conventional apparatus (Xenon Co. model 720C) with modified optics and electronics.<sup>35</sup> The emission of the flash lamps was filtered with an aqueous saturated solution of TFT in order to minimise TFT photolysis in the reaction system.<sup>18</sup>

The pH of the peroxodisulfate solutions is around 2.5 due to the acid content incorporated with the  $K_2S_2O_8$  solid batches, containing water and acid (<0.3%) as impurities.<sup>36</sup> Solutions of pH 1 and 7 were prepared by addition of  $HClO_4$  or  $KOH$ , respectively. Addition of buffers was avoided, since their components may react with  $SO_4^{\cdot-}$  radical ions.<sup>5b</sup>

In order to independently study the reactions of each of the phosphate radicals, photolysis of potassium peroxodiphosphate was performed under controlled pH conditions by phosphate buffers,<sup>7</sup> i.e., pH = (4.0 ± 0.2); (7.1 ± 0.1) or (10.1 ± 0.2), where  $H_2PO_4^{\cdot}$ ,  $HPO_4^{\cdot-}$  and  $PO_4^{\cdot 2-}$  are, respectively, the main radicals formed. The ionic strength of the solutions was within the range 0.1–0.2 M.

All experiments were carried out at (25 ± 1) °C.

Solutions of TFT were prepared by dilution of saturated aqueous solutions at 25 °C. A water solubility for TFT of  $2.14 \times 10^{-3}$  M was obtained here at 25 °C.

Product analysis was performed by gas chromatography with an HP 5890 Series II Plus chromatograph equipped with a fused silica HP5-MS GC capillary column and coupled to an HP 5972 A mass selective detector. The temperature program was 80 °C isothermal programmed to 200 °C at 10 °C min<sup>-1</sup> and held at 200 °C for 5 min. Previous to their injection in the chromatograph, the organic products were separated from the aqueous phase and concentrated in Sep-Pak C18 type cartridges and extracted with diethyl ether. Extracts were injected without derivatization. In order to achieve measurable concentration of products from the flash photolysis experiments (estimated to be of the order of  $10^{-6}$ – $10^{-5}$  M per flash), several identical batches of solutions were photolysed with three flashes each and then collected before extraction of the organic products in a cartridge.

Fluoride ions were determined with a fluoride selective electrode (Radiometer, KA-I F1052F). Absorbance was measured with a computer-controlled Cary 3 spectrophotometer.

## Acknowledgements

We thank Professor Rosa Erra-Balsells for helpful discussions. This research was partially supported by the grant numbers A-13218/1-000062, A-13359/1-000084 and A-13434/1-000105 of Fundación Antorchas (Argentina). J. A. R. thanks Consejo Nacional de Investigaciones Científicas y Técnicas (CONICET, Argentina) for a graduate studentship. D. O. M. is a research member of Comisión de Investigaciones Científicas de la Provincia de Buenos Aires (Argentina). M. C. G. is a research member of CONICET.

## References

- (a) B. C. Faust, *Environ. Sci. Technol.*, 1994, **28**, 217 A and references cited therein; (b) L. Sigg, W. Stumm, J. Zobrist and F. Zürcher, *Chimia*, 1987, **41**, 159; (c) R. E. Huie, in *Advanced Series in Physical Chemistry*, ed. J. R. Barker, World Scientific, New Jersey, 1995, vol. 3.
- G. Merga, C. T. Aravindakumar, B. S. M. Rao, H. Mohan and J. P. Mittal, *J. Chem. Soc., Faraday Trans.*, 1994, **90**, 597 and references therein.
- P. Haygarth, *Scope Newsletter in Europe*, 1997, **21**, 1.
- P. Maruthamuthu and P. Neta, *J. Phys. Chem.*, 1978, **82**, 710 and references cited therein.
- (a) J. R. Huber and E. Hayon, *J. Phys. Chem.*, 1968, **72**, 3820; (b) P. Neta, R. E. Huie and A. B. Ross, *J. Phys. Chem. Ref. Data*, 1988, **17**, 1027.
- P. Maruthamuthu and H. Taniguchi, *J. Phys. Chem.*, 1977, **81**, 1944.
- (a) L. Dogliotti and E. Hayon, *J. Phys. Chem.*, 1972, **71**, 2511; (b) E. Hayon, A. Treinin and J. Wilf, *J. Am. Chem. Soc.*, 1972, **94**, 47; (c) M.-S. Tsao and W. K. Wilmarth, *J. Phys. Chem.*, 1959, **63**, 346; (d) K. Sehested, J. Holcman, E. Bjerbakke and E. J. Hart, *J. Phys. Chem.*, 1982, **86**, 2066.
- (a) S. S. Cencione, M. C. Gonzalez and D. O. Mártire, *J. Chem. Soc., Faraday Trans.*, 1998, **94**, 2933; (b) J. A. Rosso, F. J. Rodríguez Nieto, M. C. Gonzalez and D. O. Mártire, *J. Photochem. Photobiol. A: Chemistry*, 1998, **116**, 21.
- (a) W. J. McElroy and S. J. Waygood, *J. Chem. Soc., Faraday Trans.*, 1990, **86**, 2557; (b) S. C. Choure, M. M. M. Bamatraf, B. S. M. Rao, R. Das, H. Mohan and J. P. Mittal, *J. Phys. Chem. A*, 1997, **101**, 9837.
- R. L. Lussier, W. M. Risen and J. O. Edwards, *J. Phys. Chem.*, 1970, **74**, 4039.
- J. L. Faria and S. Steenken, *J. Phys. Chem.*, 1992, **96**, 10869.
- G. L. Hug, *Nat. Stand. Ref. Data Ser., (U.S. Nat. Bur. Stand.)*, 1981, **69**.
- P. Neta, V. Madhavan, H. Zemel and R. W. Fessenden, *J. Am. Chem. Soc.*, 1977, **99**, 163.
- M. Charton, in *Progress in Physical Chemistry*, ed. R. W. Taft, Interscience, New York, 1987, vol. 16, p. 287.
- (a) S. Steenken, in *Free Radicals in Synthesis and Biology*, NATO ASI Series C - 260, ed. F. Minisci, Kluwer Academic Publishers, Dordrecht, 1989, 220; (b) G. Merga, B. S. M. Rao, H. Mohan and J. P. Mittal, *J. Phys. Chem.*, 1994, **98**, 9158.
- C. von Sonntag and H. P. Schuchmann, *Angew. Chem., Int. Ed. Engl.*, 1991, **30**, 1229.
- H. Mohan, M. Mudaliar, C. T. Aravindakumar, B. S. Rao and J. P. Mittal, *J. Chem. Soc., Perkin Trans. 2*, 1991, 1387.
- N. Karpel Vel Leitner, B. Gombert, R. Ben Abdesslem and M. Doré, *Chemosphere*, 1996, **32**, 893.
- L. S. Villata, J. A. Rosso, M. C. Gonzalez and D. O. Mártire, *J. Chem. Res. (S)*, 1997, 172.
- G. V. Buxton, C. L. Greenstock, W. P. Helman and A. B. Ross, *J. Phys. Chem. Ref. Data*, 1988, **17**, 513.
- (a) E. J. Land and M. Ebert, *Trans. Faraday Soc.*, 1967, **63**, 1181; (b) P. B. Draper, M. A. Fox, E. Pelizzetti and N. Serpone, *J. Phys. Chem.*, 1989, **93**, 1938.
- M. K. Eberhardt, *J. Phys. Chem.*, 1974, **78**, 1795.
- A. J. Swallow, in *Progress in Reaction Kinetics*, eds. K. R. Jennings and R. B. Cundall, Pergamon Press, Oxford, 1979, vol. 9.
- H. Mohan and J. P. Mittal, *J. Phys. Chem.*, 1995, **99**, 6519.
- H. Mohan and J. P. Mittal, *J. Chem. Soc., Faraday Trans.*, 1995, **91**, 2121.
- P. Neta, R. E. Huie and A. B. Ross, *J. Phys. Chem. Ref. Data*, 1990, **19**, 413.
- R. Filler, in *Trifluoromethyl Aromatic Compounds, Advances in Fluorine Chemistry*, 1970, Series 6, eds. J. C. Tatlow, R. D. Peacock, H. H. Hyman and M. Stacey, Butterworth, London, 1970 and references therein.
- W. B. Whalley, *J. Chem. Soc.*, 1949, 3016.
- J. E. Lefler, *An Introduction to Free Radicals*, John Wiley and Sons, New York, 1993, p. 121.
- P. Y. Jiang, Y. Katsumura, R. Nagishi, M. Domae, K. Ishikawa and K. Ishigure, *J. Chem. Soc., Faraday Trans.*, 1992, **88**, 1653.
- (a) R. H. Schule and G. Buzzard, *Int. J. Radiat. Phys. Chem.*, 1976, **8**, 563; (b) M. Jonsson, J. Lind, T. Reitberger, T. E. Eriksen and G. Merényi, *J. Phys. Chem.*, 1993, **97**, 8229; (c) G. E. Adams, B. D. Michael and E. J. Land, *Nature*, 1966, 294.
- (a) P. M. Sommeling, P. Mulder, R. Louw, D. V. Avila, J. Luszyk and K. U. Ingold, *J. Phys. Chem.*, 1993, **97**, 8361; (b) Z. B. Alfasi, S. Maguet and P. Neta, *J. Phys. Chem.*, 1993, **98**, 8019.
- J. K. Kochi, in *Free Radicals*, ed. J. K. Kochi, John Wiley, New York, 1993, vol. 1.
- I. I. Creaser and J. O. Edwards, *Top. Phosphorus Chem.*, 1972, **7**, 379.
- M. C. Gonzalez and D. O. Mártire, *Int. J. Chem. Kinet.*, 1997, **29**, 589.
- Riedel de Häen (Germany), personal communication.